

Precision growth index using the clustering of cosmic structures

A. Pouri,^{1,*} S. Basilakos,^{2,†} and M. Plionis^{3,4,5,‡}

¹*Academy of Athens, Research Center for Astronomy and Applied Mathematics, Soranou Efessiou 4, 11527, Athens, Greece
Faculty of Physics, Department of Astrophysics - Astronomy - Mechanics,
University of Athens, Panepistemiopolis, Athens 157 83*

²*Academy of Athens, Research Center for Astronomy and Applied Mathematics, Soranou Efessiou 4, 11527, Athens, Greece*

³*Physics Dept., Sector of Astrophysics, Astronomy & Mechanics,
Aristotle Univ. of Thessaloniki, Thessaloniki 54124, Greece*

⁴*Instituto Nacional de Astrofísica Óptica y Electrónica, 72000 Puebla, México*

⁵*IAASARS, National Observatory of Athens, P.Pendeli 15236, Greece*

We use the clustering properties of Luminous Red Galaxies (LRGs) and of SDSS rich galaxy clusters in order to constrain the growth index (γ) of the linear matter fluctuations. We perform a standard χ^2 -minimization procedure between theoretical expectations and data, followed by a joint likelihood analysis and we find a value of $\gamma = 0.54 \pm 0.03$, perfectly consistent with the expectations of the Λ CDM model, and $\Omega_{m0} = 0.30 \pm 0.01$, in excellent agreement with the latest Planck results. Our analysis provides significantly more stringent growth index constraints with respect to previous studies, as indicated by the fact that the corresponding uncertainty is only $\sim 0.06\gamma$. Finally, allowing γ to vary with redshift we find degeneracies among the model parameters, as other similar studies. In order to alleviate the degeneracy we utilize a combined statistical analysis between our clustering and literature growth data and obtain more stringent constraints with respect to other recent studies.

PACS numbers: 98.80.-k, 98.80.Bp, 98.65.Dx, 95.35.+d, 95.36.+x

I. INTRODUCTION

The statistical analysis of various cosmological data (SNIa, Cosmic Microwave Background-CMB, Baryonic Acoustic Oscillations-BAOs, Hubble parameter measurements etc) strongly suggests that we live in a spatially flat universe that consists of $\sim 4\%$ baryonic matter, $\sim 26\%$ dark matter and $\sim 70\%$ some sort of dark energy (hereafter DE) which is necessary to explain the accelerated expansion of the universe (cf. [1–7] and references therein). Although there is a common agreement regarding the ingredients of the universe, there are different views concerning the possible physical mechanism which is responsible for the cosmic acceleration. Briefly, the general path that one can follow in order to mathematically treat the accelerated expansion of the universe is to see DE either as a new field in nature or as a modification of General Relativity (see for review [8–10]).

An interesting approach to discriminate between scalar field DE and modified gravity is to use the evolution of the linear growth of matter perturbations $\delta_m(z) = \delta\rho_m/\rho_m$ [11, 12]. Specifically, a useful tool in this kind of studies is the so called growth rate of clustering, which is defined as $f(a) = \frac{d \ln D}{d \ln a} \simeq \Omega_m^\gamma(a)$, where $a(z) = (1+z)^{-1}$ is the scale factor of the universe, $\Omega_m(a)$ is the dimensionless matter density parameter, γ is the growth index and $D(a) = \delta_m(a)/\delta_m(a=1)$ is the linear growth factor scaled to unity at the present time [13, 14]. The accu-

rate determination of the growth index is considered one of the main goals of Observational Cosmology because it can be used in order to check the validity of General Relativity on cosmological scales. The basic ingredient in this approach comes from the fact that γ depends weakly on the dark energy equation of state (hereafter EoS) parameter $w(z)$ [12], implying that one can split the background expansion history, $H(z)$, constrained by geometric probes (SNIa, BAO, CMB), from the dynamical perturbations growth history.

Theoretically speaking, it has been shown that for those DE models which are within the framework of GR and have a constant EoS parameter, the growth index γ is well approximated by $\gamma \simeq \frac{3(w-1)}{6w-5}$ [12, 14–16]. In the case of the concordance Λ CDM model [$w(z) = -1$] the above formula reduces to $\gamma \approx 6/11$. Considering the braneworld model of [17] we have $\gamma \approx 11/16$ (see [12, 18–20]). Finally, for some $f(R)$ gravity models it has been found that $\gamma \simeq 0.415 - 0.21z$ for various parameter values (see [21, 22]), while for the Finsler-Randers cosmology, Basilakos & Stavrinos [23] found $\gamma \approx 9/14$.

From the large scale structure point of view, the study of the distribution of matter on large scales using different extragalactic mass tracers (galaxies, AGNs, clusters of galaxies etc) provides important constraints on structure formation theories. In particular, since gravity reflects, via gravitational instability, on the nature of clustering [13] it has been proposed to use the clustering/biasing properties of the mass tracers in constraining cosmological models (see [24–27]) as well as to test the validity of GR on extragalactic scales ([45] for a recent review see [28]).

Based on the above arguments, the aim of the current study is to place constraints on the (Ω_m, γ) parameter

*Electronic address: athpouri@uoa.gr

†Electronic address: svasil@academyofathens.gr

‡Electronic address: mplionis@auth.gr

space using the measured two point angular correlation function (hereafter ACF) of the LRGs and of SDSS-III rich clusters of galaxies. The merit of utilizing ACF data for such a task is related to the fact that we do not need to consider a fiducial cosmological model in order to derive the ACF data, as well as on the fact that the ACF is unaffected by redshift-space distortions. This is not the case for the $f(z)$ growth data that one has to initially impose a reference cosmology in order to extract the growth data [16].

The structure of the paper is as follows. In section II we present the angular correlation function data (hereafter ACF), measured for LRGs and SDSS-III galaxy clusters. In section III we discuss the theoretical angular correlation function model and basic ingredients in order to calculate it, such as the linear growth of matter perturbations, the evolution of the linear bias factor and the CDM power spectrum. The details of our methodology used to fit models to the data and our results are presented in section IV, while our main conclusions in section V.

II. ANGULAR CORRELATION FUNCTION DATA

It is well known that the two-point ACF, $w(\theta)$, is defined as the excess joint probability over random of finding two mass tracers (galaxies, AGNs, clusters) separated by an angular separation θ . Therefore by definition we have $w(\theta) = 0$ for a random distribution of sources.

In this work we use the ACF of two mass tracers; that of 2SLAQ LRGs with median redshift $z_* \simeq 0.55$, and that of relatively rich clusters of galaxies with median redshift $z_* \simeq 0.35$.

- **LRGs:** We utilize the ACF of 655775 photometrically selected LRGs from the SDSS DR5 catalogue, already estimated in [33]. This sample has been compiled using the same selection criteria as the 2dF-SDSS LRG and Quasar survey (hereafter 2SLAQ), which covers the redshift range: $0.45 < z < 0.8$. Following the original paper of [33] we use the ACF up to an angular scale of 6000'' in order to avoid the effects of BAO's. Since the aim of our paper is to put constraints on the linear growth index we also exclude small angular scales ($\theta < 120''$, which corresponds to $\leq 0.6 h^{-1}$ Mpc at z_*) where strong non-linear effects (the so-called "one-halo" term) are expected, although we do use in our theoretical modelling a mildly non-linear correction term (see also section IIIC).
- **Rich SDSS-III Clusters:** We use also in our analysis the ACF of the rich SDSS-III clusters of galaxies [29], which we estimate ourselves. We limit our analysis in the central SDSS region ($125^\circ < \text{RA} < 230^\circ$, $-3^\circ < \text{DEC} < 60^\circ$), in order to avoid the complex survey boundaries. This subsample contains in total 58631 clusters of all richnesses, while

TABLE I: The measured angular correlation function data of the 2SLAQ LRGs from [33]. We use here bootstrap errors meaning that we need to multiply the uncertainties of [33] with $\sqrt{3}$.

Index	θ''	$w(\theta)$	$\delta w(\theta)$
1	153.72	0.285	0.0061
2	230.64	0.199	0.0038
3	345.96	0.152	0.0026
4	518.94	0.113	0.0019
5	778.2	0.078	0.0018
6	1167.6	0.055	0.0012
7	1751.4	0.038	0.0011
8	2626.8	0.0226	0.0009
9	3600	0.0144	0.0008
10	4800	0.0086	0.00076
11	6000	0.0054	0.00067

we choose to use the 22144 richest galaxy clusters, i.e., those with richness class $R_{L*} \geq 15$ (defined as the ratio of total galaxy r-band luminosity within r_{200} in units of L_* , properly evolved at the estimated redshift of the cluster; see [29]). We decided to limit our analysis to the richest clusters in order to avoid the noise that could be introduced by the expected increase of spurious clusters at the lowest richness levels.

In order to measure the cluster two-point ACF we use the minimum variance estimator proposed by [30]:

$$w(\theta) = 4 \frac{N_{DD} \langle N_{RR} \rangle}{\langle N_{DR} \rangle^2} - 1 \quad (1)$$

with N_{DD} the number of cluster pairs in the interval $[\theta - \Delta\theta, \theta + \Delta\theta]$, while $\langle N_{RR} \rangle$ and $\langle N_{DR} \rangle$ are the average, over 100 random simulations with the same survey boundaries as the real data, cluster-random and random-random pairs, respectively. We also use the estimator of [31] and we find that our results remain unaltered. The uncertainties assigned to the resulting $w(\theta)$ correspond to bootstrap errors [32]:

$$\sigma_w \simeq \sqrt{3} \frac{1 + w(\theta)}{\sqrt{DD(\theta)}}. \quad (2)$$

We choose to use bootstrap uncertainties in order to reduce the effect of correlated errors, especially at the larger angular separations which are the most affected by such bin-to-bin correlations (see for example [33]). Furthermore, the largest separations could be affected by BAO's and therefore we extend our analysis up to $\theta \simeq 10000''$.

In Tables I and II we list the precise numerical values of the ACF data points with the corresponding errors that are used in our analysis.

TABLE II: The measured angular correlation function in the case of SDSS-III rich galaxy clusters.

Index	θ''	$w(\theta)$	$\delta w(\theta)$
1	362.49	0.87971	0.1270113
2	529.25	0.44467	0.0994890
3	772.72	0.29694	0.0570018
4	1128.18	0.22572	0.0396640
5	1647.17	0.14853	0.0265870
6	2404.90	0.11106	0.0162986
7	3511.21	0.07573	0.0138910
8	5126.44	0.05348	0.0093877
9	7484.71	0.03341	0.0061661

III. MODELLING THE THEORETICAL CORRELATION FUNCTION

In this section we briefly discuss the basic steps of modelling the theoretically expected ACF for the two different mass tracers used and of the evolution of bias of extragalactic mass tracers. Considering a spatially flat Friedmann-Lemaître-Robertson-Walker (FLRW) geometry, we can easily relate via the Limber's inversion equation the ACF with the two point spatial correlation function $\xi(r, z)$:

$$w(\theta) = 2 \frac{H_0}{c} \int_0^\infty \left(\frac{1}{N} \frac{dN}{dz} \right)^2 E(z) dz \int_0^\infty \xi(r, z) du, \quad (3)$$

where $1/N dN/dz$ is the normalized redshift distribution of the sources under study, which is provided by a random subsample of the source population for which redshifts (spectroscopic or photometric) are available (see section IV).

The spatial correlation function of the mass tracers is given by

$$\xi(r, z) = b^2(z) \xi_{DM}(r, z) \quad (4)$$

where $b(z)$ is the evolution of the linear bias, and ξ_{DM} is the corresponding correlation function of the underlying mass distribution which is written as

$$\xi_{DM}(r, z) = \frac{1}{2\pi^2} \int_0^\infty k^2 P(k, z) \frac{\sin(kr/a)}{(kr/a)} dk. \quad (5)$$

with $P(k, z) = D^2(z) P(k)$, and $P(k)$ denoting the power spectrum of the matter fluctuations.

The variable r corresponds to the physical separation between two sources having an angular separation, θ (in steradians). In the case of a small angle approximation the physical separation becomes

$$r \simeq a(z) (u^2 + x^2 \theta^2)^{1/2} \quad (6)$$

where u is the line-of-sight separation of any two sources and $x(z)$ is the comoving distance, given by:

$$x(z) = \frac{c}{H_0} \int_0^z \frac{dy}{E(y)}, \quad (7)$$

$E(z) = H(z)/H_0$, is the normalized Hubble parameter.

Inserting Eqs.(4), (5), (6) and $a(z) = 1/(1+z)$ into Eq.(3) and integrating over the variable u we arrive at (see also [34]) our final theoretically expected ACF:

$$w(\theta) = \frac{1}{2\pi} \int_0^\infty k^2 P(k) dk \int_0^\infty D^2(z) j(k, z, \theta) dz \quad (8)$$

with

$$j(k, z, \theta) = \frac{H_0}{c} \left(\frac{1}{N} \frac{dN}{dz} \right)^2 b^2(z) E(z) J_0(k\theta x(z)) \quad (9)$$

where J_0 is the Bessel function of zero kind, given by:

$$J_0(\omega) = \frac{2}{\pi} \int_0^\infty \sin(\omega \cosh \tau) d\tau = \frac{1}{\pi} \int_0^\pi \cos(\omega \sin \tau) d\tau \quad (10)$$

Note that the expectations for the different mass tracers enter through the bias evolution factor, $b(z)$, and the tracer redshift distribution $1/N dN/dz$.

Obviously, the dependence of ACF on gravity as well as on the different expansion models enters through the behavior of $D(z)$, which in turn depends on γ (see equation 17), and on $E(z) = H(z)/H_0$ respectively.

In the subsections below we present the different ingredients that enter in Eq.(8), namely, the linear perturbation growth rate, the bias evolution factor and the CDM power spectrum.

A. The linear growth rate, $D(a)$

Here we provide the form of the linear density perturbation growth rate, which is the ingredient through which the growth index, γ , enters in our analysis.

At sub-horizon scales the basic differential equation which describes the linear matter fluctuations ([11, 12, 35–38] and references therein) is

$$\ddot{\delta}_m + 2H\dot{\delta}_m = 4\pi G_{\text{eff}} \rho_m \delta_m \quad (11)$$

where $\rho_m \propto a^{-3}$ is the matter density, $G_{\text{eff}} = G_N Q(t)$ with G_N being the Newton's gravitational constant and the function $Q(t)$ depends on gravity. For the scalar field DE models, G_{eff} is equal to G_N , i.e., $Q(a) = 1$, while for the case of modified gravity models we have $Q(a) \neq 1$ and subsequently $G_{\text{eff}} \neq G_N$.

The growing-mode solution of equation (11) is $\delta_m \propto D(a)$, where $D(a)$ is the linear growing mode usually scaled to unity at the present time. Generally, for either modified gravity or scalar field DE we can write the following useful parametrization [12–14]

$$f(a) = \frac{d \ln \delta_m}{d \ln a} \simeq \Omega_m^\gamma(a) \quad (12)$$

where $\Omega_m(a) = \Omega_m a^{-3}/E^2(a)$. Therefore, using $d/dt = H d/d \ln a$ we express Eq.(11) in terms of $f(a)$ as:

$$\frac{df}{d \ln a} + f^2 + \left(\frac{\dot{H}}{H^2} + 2 \right) f = \frac{3}{2} Q(a) \Omega_m(a) \quad (13)$$

where for the Λ CDM expansion we have

$$\frac{\dot{H}}{H^2} + 2 = \frac{1}{2} - \frac{3}{2}w(a)[1 - \Omega_m(a)] \quad (14)$$

and $w(a) = -Q(a) = -1$. In this case the normalized Hubble parameter $E(a)$, is:

$$E(a) = [\Omega_{m0}a^{-3} + \Omega_{\Lambda0}]^{1/2} \quad (15)$$

with $\Omega_{\Lambda0} = 1 - \Omega_{m0}$ and H_0 the Hubble constant¹. As we have stated in the introduction we can separate the background expansion $H(a)$ from the growth history [12].

The parametrization of Eq.(12) greatly simplifies the numerical calculations of Eq.(11). Indeed, providing a direct integration of Eq.(12) we easily find

$$\delta_m(a, \gamma) = a(z) \exp \left[\int_{a_i}^{a(z)} \frac{dy}{y} (\Omega_m^\gamma(y) - 1) \right] \quad (16)$$

where a_i is the scale factor of the universe at which the matter component dominates the cosmic fluid (here we use $a_i \simeq 10^{-2}$). Then the linear growth factor, normalized to unity at the present epoch, is:

$$D(a) = \frac{\delta_m(a, \gamma)}{\delta_m(1, \gamma)} = \frac{a(z) \exp \left[\int_{a_i}^{a(z)} \frac{dy}{y} (\Omega_m^\gamma(y) - 1) \right]}{\exp \left[\int_{a_i}^1 \frac{dy}{y} (\Omega_m^\gamma(y) - 1) \right]}. \quad (17)$$

However, γ may not be a constant but rather evolve with redshift; $\gamma \equiv \gamma(z)$. In such a case, inserting Eq.(12) into Eq.(13) we obtain:

$$\begin{aligned} & -(1+z)\gamma' \ln(\Omega_m) + \Omega_m^\gamma + 3w(1 - \Omega_m) \left(\gamma - \frac{1}{2} \right) + \frac{1}{2} \\ & = \frac{3}{2} Q \Omega_m^{1-\gamma} \end{aligned} \quad (18)$$

where the prime denotes derivative with respect to redshift. Various functional forms of $\gamma(z)$ have been proposed in the literature [39?–41], for example:

$$\gamma(z) = \begin{cases} \gamma_0 + \gamma_1 z, & \Gamma_1\text{-parametrization} \\ \gamma_0 + \gamma_1 z/(1+z), & \Gamma_2\text{-parametrization.} \end{cases} \quad (19)$$

Using the above parametrizations and Eq.(18) evaluated at the present time ($z = 0$), one can easily obtain the parameter γ_1 in terms of γ_0

$$\gamma_1 = \frac{\Omega_{m0}^{\gamma_0} + 3w_0(\gamma_0 - \frac{1}{2})(1 - \Omega_{m0}) - \frac{3}{2}Q_0\Omega_{m0}^{1-\gamma_0} + \frac{1}{2}}{\ln \Omega_{m0}}. \quad (20)$$

Owing to the fact that the Γ_1 parametrization is valid only at relatively low redshifts ($0 \leq z \leq 0.5$), for $z > 0.5$ we utilize $\gamma = \gamma_0 + 0.5\gamma_1$. In the case of the usual Λ CDM cosmological model (ie., $Q_0 = 1$, $w_0 = -1$ and $\gamma_0^{(th)} \simeq 6/11$) with $\Omega_{m0} = 0.30$, Eq.(20) gives $\gamma_1^{(th)} \simeq -0.0459$.

B. The evolution of linear bias, $b(z)$

Here we briefly present the model that we use to trace the evolution of the linear bias factor, which reflects the relation between the overdensities of luminous and of dark matter [42, 43].

We remind the reader that biasing is considered to be statistical in nature with galaxies and clusters being identified as high peaks of an underlying, initially Gaussian, random density field. The usual paradigm is of a linear and scale-independent bias, defined as the ratio of density perturbations in the mass-tracer field to those of the underline total matter field: $b = \delta_{tr}/\delta_m$ ².

In this analysis we use the bias evolution model of [45, 46]. This generalized model is based on the linear perturbation theory and the Friedmann-Lemaître solutions of the cosmological field equations. It is valid for any DE model (scalar or geometrical) and it is given by:

$$b(z) = 1 + \frac{b_0 - 1}{D(z)} + C_2 \frac{\mathcal{J}(z)}{D(z)} \quad (21)$$

with

$$\mathcal{J}(z) = \int_0^z \frac{(1+y)}{E(y)} dy. \quad (22)$$

The constants b_0 (the bias at the present time) and C_2 depend on the host dark matter halo mass, as we have verified using Λ CDM N-body simulations (see [45]), and are given by:

$$b_0(M_h) = 0.857 \left[1 + \left(C_m \frac{M_h}{10^{14} h^{-1} M_\odot} \right)^{0.55} \right] \quad (23)$$

$$C_2(M_h) = 1.105 \left(C_m \frac{M_h}{10^{14} h^{-1} M_\odot} \right)^{0.255}, \quad (24)$$

where $C_m = \Omega_{m0}/0.27$.

C. CDM Power Spectrum, $P(k)$

The CDM power spectrum is given by $P(k) = P_0 k^n T^2(k)$, where $T(k)$ is the CDM transfer function and

¹ For the comoving distance and for the dark matter halo mass we use the traditional parametrization $H_0 = 100h \text{ km/s/Mpc}$. Of course, when we treat the power spectrum shape parameter Γ we utilize $h \equiv \bar{h} = 0.68$ [7].

² We would like to point that up to galaxy cluster scales the fluctuations of the metric do not introduce a significant scale dependence in the growth factor [44] and in the linear bias [45].

$n \simeq 0.9671$ following the recent reanalysis of the Planck data by Spergel et al. [7]. Regarding $T(k)$, we use two different functional forms namely, that of Bardeen et al. [43] and of Eisenstein & Hu [47].

The [43] is given by:

$$T(k) = C_q \left[1 + 3.89q + (16.1q)^2 + (5.46q)^3 + (6.71q)^4 \right]^{-1/4} \quad (25)$$

where $C_q = \frac{\ln(1+2.34q)}{2.34q}$ and $q \equiv \frac{k}{\Gamma}$. Here Γ is the shape parameter, given according to [48] as:

$$\Gamma = \Omega_{m0} \tilde{h} \exp(-\Omega_{b0} - \sqrt{2\tilde{h}} \Omega_{b0}/\Omega_{m0}). \quad (26)$$

The value of Γ , which is kept constant throughout the model fitting procedure, is estimated using the Planck results of Spergel et al. [7]³ namely, $\Omega_{b0} = 0.022197\tilde{h}^{-2}$, $\tilde{h} = 0.68$ and $\Omega_{m0} = 0.30$. The alternative transfer function used is that of [47]:

$$T(k) = \frac{L_0}{L_0 + C_0 q^2} \quad (27)$$

where $L_0 = \ln(2e + 1.8q)$, $e = 2.718$ and $C_0 = 14.2 + \frac{731}{1+62.5q}$.

Also, the rms fluctuations of the linear density field on mass scale M_h is:

$$\sigma(M_h, z) = \left[\frac{D^2(z)}{2\pi^2} \int_0^\infty k^2 P(k) W^2(kR) dk \right]^{1/2}, \quad (28)$$

where $W(kR) = 3(\text{sinc}kR - kR\text{cos}kR)/(kR)^3$ and $R = (3M_h/4\pi\rho_0)^{1/3}$ with ρ_0 denotes the mean matter density of the universe at the present time ($\rho_0 = 2.78 \times 10^{11} \Omega_{m0} h^2 M_\odot \text{Mpc}^{-3}$). To this end, the normalization of the power spectrum is given by:

$$P_0 = 2\pi^2 \sigma_8^2 \left[\int_0^\infty T^2(k) k^{n+2} W^2(kR_8) dk \right]^{-1} \quad (29)$$

where $\sigma_8 \equiv \sigma(R_8, 0)$ is the rms mass fluctuation on $R_8 = 8h^{-1}$ Mpc scales and for which we use the Planck value of $\sigma_8 = 0.817$ [7].

Finally, we would like to stress that we have taken into account the non-linear corrections by using the corresponding fitting formula introduced by [49], for the Λ CDM model (see also [50, 51]). In their fitting formula there is one relatively free parameter, which is the slope of the power spectrum at the relevant scales, because the CDM power spectrum curves slowly and thus it varies as a function of scale according to: $n_{\text{eff}} = d\ln P/d\ln k$.

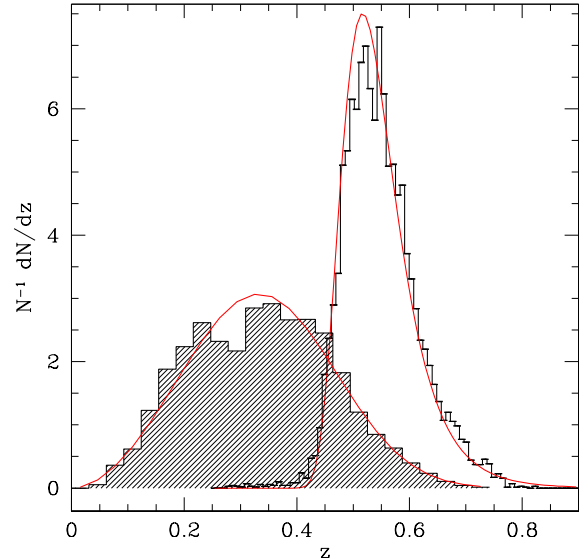


FIG. 1: The normalized photometric redshift distribution of our subsample of the SDSS-III rich galaxy clusters (hatched histogram) and of the 2SLAQ LRG galaxies. The red continuous lines are their corresponding best fits according to Eq.30.

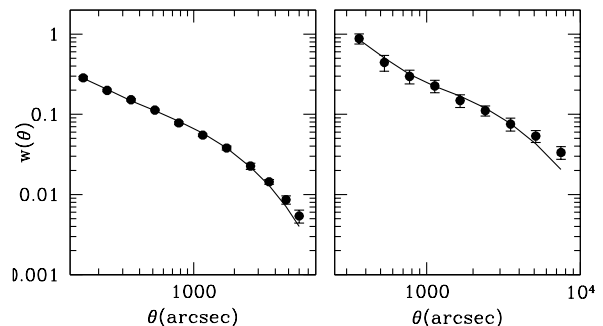


FIG. 2: Comparison of the observed (solid points) and theoretical angular correlation function. The left and right panels correspond to the 2SLAQ LRGs and SDSS-III rich galaxy clusters, respectively. In the case of clusters, the deviation from the expectations at large angular separations occurs approximately at the expected BAO scale ($\sim 10000''$).

IV. FITTING THEORETICAL MODELS TO THE DATA

In this section we implement a standard χ^2 minimization statistical analysis in order to provide constraints either in the (Ω_{m0}, γ) parameter space, or for $\gamma(z)$.

An important ingredient that is necessary in Eq.(3), in order to relate the spatial to the angular 2-point correlation functions, is the tracer redshift distribution. For the SDSS-III clusters as well as for the LRGs we use a model of their photometric redshift distribution, which we then insert in Eq.(3). The model redshift distribution is given

³ We use the Planck priors provided by Spergel et al. [7] in order to avoid possible systematics on the cosmological parameters which are related to the problematic (according to Spergel et al.) 217GHz \times 217GHz detector. However, at the end of the analysis we provide results based on the Planck results of Ade et al. [6].

TABLE III: Results in the Ω_{m0}, γ parameter space for the different $T(k)$.

$T(k)$	Ω_{m0}	γ	$M_h/10^{13}M_\odot$	n_{eff}	$\chi^2_{t,\text{min}}/df$
LRGs					
Bardeen	0.30 ± 0.01	0.54 ± 0.04	$1.68^{+0.08}_{-0.04}$	$0.20^{+0.25}_{-0.10}$	9.10/7
Hu	0.30 ± 0.01	0.54 ± 0.04	1.80 ± 0.08	0.50 ± 0.2	9.20/7
SDSS-III Clusters					
Bardeen	0.27 ± 0.03	$0.48^{+0.12}_{-0.06}$	60.2 ± 7.0	$-0.90^{+0.44}_{-0.22}$	5.53/5
Hu	0.27 ± 0.04	$0.48^{+0.12}_{-0.08}$	62.8 ± 7.2	$-0.80^{+0.44}_{-0.24}$	5.43/5
Joint LRGs+Clusters					
Bardeen	0.30 ± 0.01	0.54 ± 0.03			16.09/18
Hu	0.30 ± 0.01	0.54 ± 0.03			16.06/18

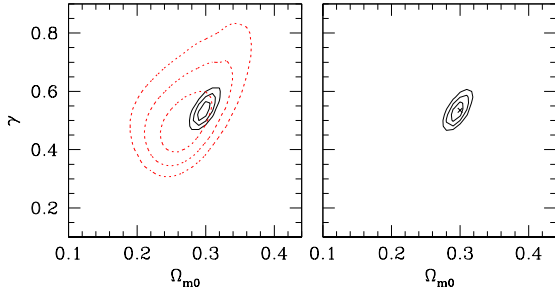


FIG. 3: Likelihood contours for $\Delta\chi^2 = \chi^2 - \chi^2_{\text{min}}$ equal to 2.32, 6.18 and 11.83, corresponding to 1σ , 2σ and 3σ confidence levels, in the (Ω_{m0}, γ) plane using the Eisenstein & Hu [47] transfer function and the [45, 46] bias model. *Left Panel:* The solid and the red dashed contours correspond to LRGs and SDSS clusters respectively. *Right Panel:* The solid curves represent the joint likelihood contours. The best fit solution $(\Omega_{m0}, \gamma) = (0.30, 0.54)$ is represented by the cross. Note that using the Bardeen et al. [43] transfer function we find the same results.

by fitting the following useful formula to the data:

$$\frac{dN}{dz} \propto \left(\frac{z}{z_*}\right)^{(a+2)} e^{-\left(\frac{z}{z_*}\right)^\beta}. \quad (30)$$

This fitting formula provides us with the relevant parameters:

$$(a, \beta, z_*) = \begin{cases} -0.08, 3.08, 0.388 & \text{SDSS-III clusters} \\ -15.53, -8.03, 0.55 & \text{2SLAQ LRGs} \end{cases} \quad (31)$$

where z_* is the characteristic depth of the subsample studied. In Fig.1, we present the estimated normalized redshift distribution $(\frac{1}{N} \frac{dN}{dz})$ and the corresponding continuous fit provided by Eq.(30).

We are now set to compare, using a χ^2 minimization procedure, the measured 2SLAQ LRGs and SDSS-III rich clusters angular correlation functions with the predictions of different spatially flat Λ cosmological models.

The corresponding χ^2 is defined as:

$$\chi_D^2(\mathbf{p}_1, \mathbf{p}_{2,D}) = \sum_{i=1}^{N_D} \frac{[w_{\text{th}}(\theta_i, \mathbf{p}_1, \mathbf{p}_{2,D}) - w_D(\theta_i)]^2}{\sigma_i^2}. \quad (32)$$

Note, that D stands for the data used ($D = \text{LRGs or CL}$), σ_i is the uncertainty of the observed angular correlation function and N_D corresponds to the number of data points used in the fitting, with $N_{\text{LRGs}} = 11$ and $N_{\text{CL}} = 9$ (see Tables I and II). Note that the uncertainty of each fitted parameter will be estimated after marginalizing one parameter over the other, providing as its uncertainty the range for which $\Delta\chi^2 \leq 1\sigma$. Such a definition, however, may hide the extent of a possible degeneracy between the fitted parameters and thus it is important to visualize the solution space, as indicated in the relevant contour figures. As a consistency check we have used the inverse of the Fisher matrix, called the covariance matrix, and we find similar uncertainties to those provided by the marginalization method. Since the errors of the Fisher matrix approach by definition are symmetric we have decided to use the marginalization approach.

In Fig. 2, we present the observed $w(\theta)$ for the 2SLAQ LRGs (left panel) and for the SDSS-III clusters (right panel), with the best fit model of the angular correlation function provided by Eq.(8) and the minimization procedure discussed below.

The statistical vectors \mathbf{p}_1 and $\mathbf{p}_{2,D}$ provide the essential free parameters that enter in the theoretical expectation. The "cosmo-gravity" \mathbf{p}_1 vector contains those free parameters which are related to the expansion and gravity. For the case of constant γ it is defined as: $\mathbf{p}_1 = (\Omega_{m0}, \gamma, \sigma_8)$, and for the case of evolving γ , as: $\mathbf{p}_1 = (\Omega_{m0}, \gamma_0, \gamma_1, \sigma_8)$. The $\mathbf{p}_{2,D} = (M_h, n_{\text{eff}})$ vector is associated with the environment of the dark matter halo in which the extragalactic mass tracers (in our case LRGs and SDSS rich clusters) live.

After the determination of $\mathbf{p}_{2,D}$ from each set of data ($D = \text{LRGs and CL}$), we can perform a joint likelihood analysis. Generally, since likelihoods are defined as $\mathcal{L} \propto \exp(-\chi^2/2)$, one has that the joint likelihood is given by:

$$\mathcal{L}_t(\mathbf{p}_1) = \mathcal{L}_{\text{LRGs}}(\mathbf{p}_1, \mathbf{p}_{2,\text{LRGs}}) \times \mathcal{L}_{\text{CL}}(\mathbf{p}_1, \mathbf{p}_{2,\text{CL}}), \quad (33)$$

which is equivalent to:

$$\chi_t^2(\mathbf{p}_1) = \chi_{\text{LRGs}}^2(\mathbf{p}_1, \mathbf{p}_{2,\text{LRGs}}) + \chi_{\text{CL}}^2(\mathbf{p}_1, \mathbf{p}_{2,\text{CL}}). \quad (34)$$

A. Constraints on (Ω_{m0}, γ)

In our analysis we have set $\sigma_8 = 0.817$ and thus $\mathbf{p}_1 = (\Omega_{m0}, \gamma, 0.817)$. However, in order to use the σ_8 prior properly along the γ -chain we rescale the values of σ_8 by

$$\sigma_{8,\gamma} = \sigma_8 \frac{\delta_m(1, \gamma)}{\delta_m(1, \gamma_\Lambda^{(th)})} \quad (35)$$

where $\delta_m(a, \gamma)$ is given by Eq.(16).

In Table III we present our resulting parameter constraints separately for the case of the LRGs and the SDSS-III as well as for their joint analysis. The results are separated to those for each of the two transfer functions under study.

A first general result is that the two transfer functions used provide extremely similar cosmo-gravity results. Secondly, we would like to mention that the χ_{min}^2 for the LRGs, resulting in a reduced value of $\chi_{\text{min}}^2/df \sim 9/7$ while the corresponding χ_{min}^2/df value for the SDSS clusters is $\sim 5.5/5$.

In Figure 3 we present the 1σ , 2σ and 3σ confidence contours in the (Ω_{m0}, γ) plane for both 2SLAQ LRGs and SDSS-III clusters of galaxies (left panel), while in the right panel we present the corresponding contours of the joint-analysis. These results are based on the transfer function of Ref.[47]. It is clear that the results of the joint analysis are dominated by the LRGs although the combination of LRGs with galaxy clusters slightly tightens the constraints on (Ω_{m0}, γ) . As it can also be seen from Table III, in the case of LRGs as well as for the joint case, $\Omega_{m0} = 0.30 \pm 0.01$, which is in a very good agreement with the one found by Planck [7], and the derived value of $\gamma = 0.54 \pm 0.03$ coincides with the theoretically expected Λ CDM value. Note that the $\chi_{t,\text{min}}^2$ of the overall statistical analysis is ~ 16.1 for 18 degrees of freedom.

With respect to other recent studies, our best fit values of γ are in agreement, within 1σ errors, to that of [53] (see also [52]) who found $\gamma = 0.597 \pm 0.046$, using a combined statistical analysis of expansion and growth data (SNIa/BAOs/CMB_{shift}/ $f\sigma_8$). However, our joint Ω_{m0} value is somewhat greater (within 2.4σ uncertainties), from the derived value of [53], $\Omega_{m0} = 0.272 \pm 0.003^4$.

In order to appreciate the great effort in the recent years to estimate jointly Ω_{m0} and γ and the relative strength and precision of the different methods, we present a summary of relevant literature results in Table IV. It appears unavoidable to conclude that current data

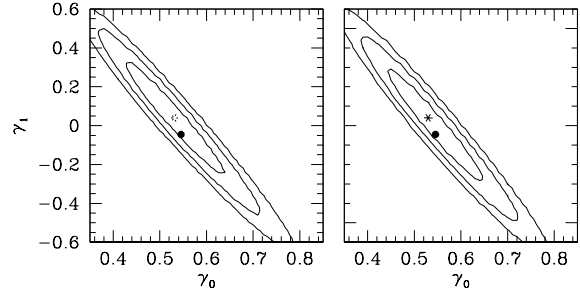


FIG. 4: The joint 2SLAQ (LRGs) galaxy $w(\theta)$ and $f\sigma_8$ likelihood contours (solid curves) in the (γ_0, γ_1) plane (using the Planck priors of Spergel et al. [7]). The left and right panels show the results based on the Γ_1 and Γ_2 parametrizations respectively. The crosses correspond to the best fit parameters. We also show the theoretical Λ CDM $(\gamma_0^{(th)}, \gamma_1^{(th)})$ values (solid points) given in section IVB.

favor, within a 1σ uncertainty, the theoretically predicted value of $\gamma_\Lambda^{(th)} \simeq 6/11$. Secondly, the quality and quantity of the cosmological and dynamical (growth and the like) data as well as methodologies have greatly improved in recent years. For example, since the first measurement of [54], the error budget of the growth index has been decreased by a factor of ~ 120 with respect to best fit value of the current work. It is also important to note that using only the clustering properties of the large scale structures (2SLAQ LRGs and rich SDSS clusters) we have managed to significantly reduce the growth index uncertainty, namely $\sigma_\gamma/\gamma \sim 6\%$ and thus producing the strongest (to our knowledge) existing joint constraints on γ .

B. Constraints on $\gamma(z)$

In order to perform a consistent minimization procedure in the (γ_0, γ_1) parameter space, we need again to rescale σ_8 to that relevant to each model. This is achieved by the following:

$$\sigma_{8,\gamma} = \sigma_8 \frac{\delta_m(1, \gamma_0, \gamma_1)}{\delta_m(1, \gamma_0^{(th)}, \gamma_1^{(th)})}. \quad (36)$$

Following the considerations discussed in the previous section and for the sake of simplicity the "cosmo-gravity" vector becomes $\mathbf{p}_1 = (0.30, \gamma_0, \gamma_1, 0.817)$, where we have marginalized again the overall likelihood analysis over the environmental vectors $\mathbf{p}_{2,\text{LRGs}}$ and $\mathbf{p}_{2,\text{CL}}$. Notice, that we sample $\gamma_0 \in [0.35, 0.85]$ in steps of 0.01 and $\gamma_1 \in [-0.6, 0.6]$ in steps of 0.01.

Our minimization analysis provided strongly degenerate results between γ_0 and γ_1 , rendering impossible to put any significant constraints on their values. Therefore, we attempt to rectify this by additionally utilizing

⁴ Nesseris et al. [53] imposed $\sigma_8 = 0.80$.

TABLE IV: Literature growth results for the Λ CDM cosmological model. The last line corresponds to our results. Similar to [52] results can be also found in [53].

Data used	Ω_{m0}	γ	References
galaxy data from 2dFGRS	0.30 ± 0.02	$0.60^{+0.40}_{-0.30}$	[54]
old $f(z)$ growth data	0.30	$0.674^{+0.195}_{-0.169}$	[16]
old $f(z)$ growth data	0.273 ± 0.015	$0.64^{+0.17}_{-0.15}$	[19]
X-ray cluster luminosity function+ f_{gas}	$0.214^{+0.036}_{-0.041}$	$0.42^{+0.20}_{-0.16}$	[55]
WMAP+SN Ia+MCMC	0.25	0.584 ± 0.112	[56]
old+new $f(z)$ growth data	0.273 ± 0.011	$0.586^{+0.079}_{-0.074}$	[41]
$f\sigma_8$ growth data	0.259 ± 0.045	0.619 ± 0.054	[57]
$f\sigma_8$ growth data	0.273	0.602 ± 0.055	[58]
old+new $f(z)$ growth data	0.273	0.58 ± 0.04	[63]
$f\sigma_8$ growth data+(SN Ia, BAOs, CMB _{shift})	0.272 ± 0.003	0.597 ± 0.046	[52, 53]
CMASS DR9+ other $f\sigma_8$	0.308 ± 0.022	0.64 ± 0.05	[59]
cl+CMB+gal+SN Ia+BAO	0.284 ± 0.012	0.618 ± 0.062	[60]
Lensing + $f\sigma_8$ growth data	0.256 ± 0.023	0.52 ± 0.09	[61]
CMB+clustering of Baryon Oscillation Spec. Survey	0.30 ± 0.01	0.69 ± 0.15	[62]
Clustering of LRGs+SDSS-III clusters	0.30 ± 0.01	0.54 ± 0.03	Our study

TABLE V: Literature (γ_0, γ_1) constraints. The bold phase lines correspond to the present analysis.

Parametrization Model	γ_0	γ_1	Reference
$\Gamma_1 : \gamma(z) = \gamma_0 + \gamma_1 z$	0.77 ± 0.29	-0.38 ± 0.85	[16]
	0.774	-0.556	[20]
	$0.49^{+0.12}_{-0.11}$	$0.305^{+0.345}_{-0.318}$	[41]
	0.48 ± 0.07	0.32 ± 0.20	[63]
	$0.40^{+0.086}_{-0.080}$	0.603 ± 0.241	[58]
	0.567 ± 0.066	0.116 ± 0.19	[52, 53]
	0.530 ± 0.04	0.04 ± 0.11	Our study
$\Gamma_2 : \gamma(z) = \gamma_0 + \gamma_1 z/(1+z)$	$0.92^{+1.56}_{-1.26}$	$-1.49^{+6.86}_{-6.08}$	[64]
	$0.461^{+0.12}_{-0.11}$	$0.513^{+0.448}_{-0.414}$	[41]
	0.46 ± 0.09	0.55 ± 0.36	[63]
	$0.345^{+0.085}_{-0.080}$	1.006 ± 0.314	[58]
	0.561 ± 0.068	0.183 ± 0.26	[52, 53]
	0.530 ± 0.03	0.04 ± 0.11	Our study

the recent $f\sigma_8$ growth data (as collected by [52]) which contain 16 entries. Since different authors have estimated $f\sigma_8$ using different cosmologies, we need to convert them to the same cosmological background in order to be able to utilize them consistently. Note that as a background cosmology we choose $(\Omega_{m0}, \sigma_8) = (0.30, 0.817)$, which is in agreement with Planck results [7].

Specifically, we wish to translate the value of growth data $f\sigma_8$ from a reference cosmological model, say Ref, to the background cosmology. The definition of $f(z)$ and $\sigma_8(z)$ simply implies a correction factor:

$$C_f = \frac{f\sigma_{8,\text{obs}}}{f\sigma_{8,\text{obs}}^{\text{Ref}}} = \left[\frac{\Omega_m(z)}{\Omega_m^{\text{Ref}}(z)} \right]^{\gamma(z)} \frac{\sigma_8 D(\Omega_{m0}, z)}{\sigma_8^{\text{Ref}} D(\Omega_{m0}^{\text{Ref}}, z)}. \quad (37)$$

Then we implement a joint statistical analysis, involving

the 2SLAQ LRGs clustering data and the growth data⁵

$$\chi_t^2(\mathbf{p}_1) = \chi_{\text{LRGs}}^2(\mathbf{p}_1, \mathbf{p}_2, \text{LRGs}) + \chi_{\text{gr}}^2(\mathbf{p}_1), \quad (38)$$

with

$$\chi_{\text{gr}}^2(\mathbf{p}_1) = \sum_{i=1}^{16} \left[\frac{C_f(z_i, \mathbf{p}_1) f\sigma_{8,\text{obs}}^{\text{Ref}}(z_i) - f\sigma_8(z_i, \mathbf{p}_1)}{C_f(z_i, \mathbf{p}_1) \sigma_i^{\text{Ref}}} \right]^2 \quad (39)$$

where

$$f\sigma_8(z, \mathbf{p}_1) = \sigma_8 D(z) \Omega_m(z)^{\gamma(z)}, \quad (40)$$

σ_i^{Ref} is the observed growth rate uncertainty. The $f\sigma_{8,\text{obs}}^{\text{Ref}}$ data and the corresponding uncertainties can be found in Table V of [52].

⁵ We decide to exclude from the statistical analysis the SDSS III cluster data due to large errors with respect to the LRGs clustering and growth data.

In Fig.4 we plot the results of our statistical analysis in the (γ_0, γ_1) plane for the Eisenstein & Hu [47] transfer function, since we have verified that using Bardeen et al. [43] transfer function we get similar contours. The left panel shows the Γ_1 parametrization while the right panel the Γ_2 parametrization.

The theoretical $(\gamma_0^{(th)}, \gamma_1^{(th)})$ Λ CDM values (see above) are indicated by the solid points while the stars represent our best fit values. It is evident that the predicted Λ CDM $(\gamma_0^{(th)}, \gamma_1^{(th)})$ values of both parametrizations are close to the best fit parameters ($\Delta\chi^2 \simeq 1.6$; see solid points in Fig. 4). Concerning the best fit parameters we obtain:

- for the Γ_1 parametrization: (i) in the case of Bardeen et al. [43] transfer function we have $\chi_{t,\min}^2/df = 16.4/25$, $\gamma_0 = 0.54 \pm 0.04$, $\gamma_1 = 0.04 \pm 0.11$, and (ii) using the transfer function the Eisenstein & Hu [47] we find $\gamma_0 = 0.53 \pm 0.04$, $\gamma_1 = 0.04 \pm 0.11$. In both cases the reduced $\chi_{t,\min}^2/df$ is $\simeq 16.4/25$.
- for the Γ_2 parametrization: similarly, we obtain (i) $\chi_{t,\min}^2/df = 16.5/25$, $\gamma_0 = 0.56 \pm 0.03$, $\gamma_1 = -0.04 \pm 0.11$ and (ii) $\gamma_0 = 0.53 \pm 0.03$, $\gamma_1 = 0.04 \pm 0.11$ with $\chi_{t,\min}^2/df \simeq 16.5/25$.

Finally, comparing the contours of Fig.4 with literature results (for the corresponding Refs. see Table V) we find that indeed we have managed to reduce significantly the area of $\gamma_0 - \gamma_1$ contours, increasing the Figure of Merit by $\sim 30\%$, with respect to that of the joint SNIa/BAOs/CMB_{shift}/ $f\sigma_8$ analysis [52, 53]. Also, in Table V, one may see a more compact presentation of our results including literature best fit (γ_0, γ_1) values.

C. Using the priors provided by the Planck team

In order to complete the current study we repeat our analysis by using those priors derived originally by the Planck team [6], namely

$$(\Omega_{b0}, \tilde{h}, n, \sigma_8) = (0.02207\tilde{h}^{-2}, 0.674, 0.9616, 0.834)$$

with $\Omega_{m0} = 0.315$. Since, we have found that the results remain mostly unaffected by using the two different forms of $T(k)$, we use here the form of Ref.[47]. In brief we find:

- in the case of a constant γ the overall likelihood function peaks at $(\Omega_{m0}, \gamma) = (0.31 \pm 0.01, 0.52 \pm 0.02)$ with $\chi_{t,\min}^2/df \simeq 16.4/18$. The corresponding environmental vectors are $\mathbf{p}_{2,\text{LRGs}} = (1.56^{+0.08}_{-0.04} \times 10^{13} h^{-1} M_\odot, 0.75 \pm 0.20)$ and $\mathbf{p}_{2,\text{CL}} = (57.8^{+6.8}_{-6.4} \times 10^{13} h^{-1} M_\odot, -0.65^{+0.45}_{-0.25})$.
- in the case of Γ_1 parametrization: $\chi_{t,\min}^2/df = 18/25$, $\gamma_0 = 0.52 \pm 0.04$, $\gamma_1 = 0 \pm 0.10$.

- in the case of Γ_2 parametrization: $\chi_{t,\min}^2/df = 17.9/25$, $\gamma_0 = 0.54 \pm 0.04$, $\gamma_1 = -0.06 \pm 0.12$.

V. CONCLUSIONS

In the epoch of intense cosmological studies aimed at testing the validity of general relativity on extragalactic scales, it is very important to minimize the amount of priors needed to successfully complete such an effort. One such prior is the growth index and its measurement at the $\sim 1\%$ accuracy level has been proposed as a necessary step for checking possible departures from general relativity at cosmological scales [28]. Therefore, it is of central importance to have independent determinations of γ , because this will help to control the systematic effects that possibly affect individual methods and tracers of the growth of matter perturbations.

In this study we use the clustering properties of the 2SLAQ Luminous Red Galaxies together with the SDSS-III rich clusters of galaxies in order to constrain the growth index of matter perturbations. The results of the two analyzes are used in a joint likelihood fitting procedure, and although the LRG result dominates the joint solution, the SDSS-III cluster results help reduce the parameter uncertainties. The outcome constraints are: $(\Omega_{m0}, \gamma) = (0.30 \pm 0.01, 0.54 \pm 0.03)$, which are the strongest (to our knowledge) joint constraints appearing in the literature. Also, we check that our growth results are quite robust against the choice of the transfer function of the power spectrum and the Planck priors which are available in the literature [6, 7].

Finally, considering a time varying growth index: $\gamma(z) = \gamma_0 + \gamma_1 X(z)$, [with $X(z) = z$ or $X(z) = z/(1+z)$] we find, as all similar studies, that γ_1 and γ_0 are degenerate. In order to alleviate this degeneracy we include in a joint statistical analysis the recent growth data and thus manage to put tighter constraints on γ_0 . Although, we have reduced significantly the γ_1 uncertainty with respect to previous studies, the corresponding error bars remain quite large. Future, dynamical data are expected to improve even further the relevant constraints (especially on γ_1) and thus the validity of GR on cosmological scales will be effectively tested.

Acknowledgments

AP acknowledges financial support under the Academy of Athens: *Fellowship for Astrophysics* grant 2005-49878. SB also acknowledges support by the Research Center for Astronomy of the Academy of Athens in the context of the program “*Tracing the Cosmic Acceleration*”.

-
- [1] M. Hicken et al., *Astrophys. J.*, **700**, 1097 (2009)
- [2] E. Komatsu et al., *Astrophys. J. Supp.*, **192**, 18 (2011)
- [3] C. Blake et al., *Mon. Not. Roy. Soc.*, **418**, 1707 (2011)
- [4] G. Hinshaw et al., *Astrophys. J. Supp.*, **208**, 19 (2013)
- [5] O. Farooq, D. Mania and B. Ratra, *Astrophys. J.*, **764**, 138 (2013).
- [6] P. A. R. Ade et al., (Planck Collaboration), arXiv:1303.5076 (2013)
- [7] D. Spergel, R. Flauger and R. Hlozek, arXiv:1312.3313 (2013)
- [8] E. J. Copeland, M. Sami and S. Tsujikawa, *Int. J. of Mod. Phys. D.*, **15**, 1753 (2006)
- [9] R. R. Caldwell and M. Kamionkowski, *Ann. Rev. Nucl. Part. Sci.*, **59**, 397 (2009)
- [10] L. Amendola and S. Tsujikawa, *Dark Energy: Theory and Observations*, Cambridge University Press, Cambridge UK (2010)
- [11] E. V. Linder, *Phys. Rev. D.*, **70**, 023511 (2004)
- [12] E. V. Linder and R. N. Cahn, *Astrop. Phys.*, **28**, 481 (2007)
- [13] P. J. E. Peebles, “Principles of Physical Cosmology”, Princeton University Press, Princeton New Jersey (1993)
- [14] L. Wang and P. J. Steinhardt, *Astrophys. J.*, **508**, 483 (1998)
- [15] V. Silveira and I. Waga, *Phys. Rev. D.*, **50**, 4890 (1994)
- [16] S. Nesseris and L. Perivolaropoulos, *Phys. Rev. D.*, **77**, 023504 (2008)
- [17] G. Dvali, G. Gabadadze and M. Porrati, *Phys. Lett. B.*, **485**, 208 (2000)
- [18] H. Wei, *Phys. Lett. B.*, **664**, 1 (2008)
- [19] Y. Gong, *Phys. Rev. D.*, **78**, 123010 (2008)
- [20] X. Fu, P. Wu and H. Yu, *Phys. Lett. B.*, **677**, 12 (2009)
- [21] R. Gannouji, B. Moraes and D. Polarski, *JCAP*, **2**, 34 (2009)
- [22] S. Tsujikawa, R. Gannouji, B. Moraes and D. Polarski, *Phys. Rev. D.*, **80**, 084044 (2009)
- [23] S. Basilakos and P. Stavrinos, *Phys. Rev. D.*, **87**, 043506 (2013)
- [24] T. Matsubara, *Astrophys. J.*, **615**, 573 (2004)
- [25] S. Basilakos and M. Plionis, *Mon. Not. Roy. Soc.*, **360**, L35 (2005)
- [26] S. Basilakos and M. Plionis, *Astrophys. J.*, **650**, L1 (2006)
- [27] M. Krumpke, T. Miyaji and A. L. Coil, arXiv:1308.5976 (2013)
- [28] R. Bean et al., arXiv:1309.5385 (2013)
- [29] Z. L. Wen, J. L. Han and F. S. Liu, *VizieR Online Data Catalog*, **219**, 90034 (2012)
- [30] A. J. S. Hamilton, *Astrophys. J.*, **417**, 19 (1993)
- [31] S. D. Landy, & A. S. Szalay, *Astrophys. J.*, **412**, 64 (1993)
- [32] H. J. Mo, Y. P. Jing and G. Börner, *Astrophys. J.*, **392**, 452 (1992)
- [33] U. Sawangwit et al., *Mon. Not. Roy. Soc.*, **416**, 3033 (2011)
- [34] C. M. Cress and M. Kamionkowski, *Mon. Not. Roy. Soc.*, **297**, 486 (1998)
- [35] A. Lue, R. Scoccimarro and G. D. Starkman, *Phys. Rev. D.*, **69**, 124015 (2004)
- [36] H. F. Stabenau and B. Jain, *Phys. Rev. D.*, **74**, 084007 (2006)
- [37] P. J. Uzan, *Gen. Rel. Grav.*, **39**, 307 (2007)
- [38] S. Tsujikawa, K. Uddin and R. Tavakol, *Phys. Rev. D.*, **77**, 043007 (2008)
- [39] D. Polarski and R. Gannouji, *Phys. Lett. B.*, **660**, 439 (2008)
- [40] A. B. Belloso, J. Garcia-Bellido and D. Sapone, *JCAP*, **10**, 10 (2011)
- [41] S. Basilakos, *Intern. Journal of Modern Physics D*, **21**, 1250064 (2012)
- [42] N. Kaiser, *Astrophys. J. L.*, **284**, L9 (1984)
- [43] J. M. Bardeen, J. R. Bond, N. Kaiser and A. S. Szalay, *Astrophys. J.*, **304**, 15 (1986)
- [44] J. B. Dent, S. Dutta and L. Perivolaropoulos, *Phys. Rev. D.*, **80**, 023514 (2009)
- [45] S. Basilakos, J. B. Dent, S. Dutta, L. Perivolaropoulos and M. Plionis, *Phys. Rev. D.*, **85**, 123501 (2012)
- [46] S. Basilakos, M. Plionis and A. Pouri, *Phys. Rev. D.*, **83**, 123525 (2011)
- [47] D. J. Eisenstein and W. Hu, *Astrophys. J.*, **496**, 605 (1998)
- [48] N. Sugiyama, *Astrophys. J. Supp.*, **100**, 281 (1995)
- [49] J. A. Peacock and S. J. Dodds, *Mon. Not. Roy. Soc.*, **267**, 1020 (1994)
- [50] R. E. Smith et al., *Mon. Not. Roy. Soc.*, **341**, 1311 (2003)
- [51] L. M. Widrow, P. J. Elahi, R. J. Thacker, M. Richardson and E. Scannapieco, *Mon. Not. Roy. Soc.*, **397**, 1275 (2009)
- [52] S. Basilakos, S. Nesseris and L. Perivolaropoulos, *Phys. Rev. D.*, **87**, 123529 (2013)
- [53] S. Nesseris, S. Basilakos, E. N. Saridakis and L. Perivolaropoulos, *Phys. Rev. D.*, **88**, 103010, (2013)
- [54] C. di Porto and L. Amendola, *Phys. Rev. D.*, **77**, 083508 (2008)
- [55] D. Rapetti, S. W. Allen, A. Mantz and H. Ebeling, *Mon. Not. Roy. Soc.*, **406**, 1796 (2010)
- [56] L. Samushia, W. J. Percival and A. Raccanelli, *Mon. Not. Roy. Soc.*, **420**, 2102 (2012)
- [57] M. J. Hudson and S. J. Turnbull, *Astrophys. J. Lett.*, **751**, L30 (2012)
- [58] S. Basilakos and A. Pouri, *Mon. Not. Roy. Soc.*, **423**, 3761 (2012)
- [59] L. Samushia et al., *Mon. Not. Roy. Soc.*, **429**, 1514 (2013)
- [60] D. Rapetti, C. Blake, S. W. Allen, A. Mantz, D. Parkinson and F. Beutler, *Mon. Not. Roy. Soc.*, **432**, 973 (2013)
- [61] F. Simpson et al., *Mon. Not. Roy. Soc.*, **429**, 2249 (2013)
- [62] A. G. Sanchez, et al., arXiv:1312.4854 (2014)
- [63] S. Lee, arXiv: 1205.6304 (2012)
- [64] J. Dossett, M. Ishak, J. Moldenhauer, Y. Gong, and A. Wang, *JCAP*, **4**, 22 (2010)